

Calibration of stochastic volatility models via second order approximation: the Heston model case

Elisa Alòs*

Departament d'Economia i Empresa
Universitat Pompeu Fabra and
Barcelona Graduate School of Economics
elisa.alos@upf.edu

Rafael De Santiago†

Department of Managerial Decision Sciences
IESE Business School
rsantiago@iese.edu

Josep Vives‡

Departament de Probabilitat, Lògica i Estadística and
Institut de Matemàtica de la Universitat de Barcelona (IMUB)
Universitat de Barcelona
josep.vives@ub.edu

October 22, 2012

Abstract

Using a suitable Hull and White type formula we develop a methodology to obtain a second order approximation to the implied volatility for very short maturities. Using this approximation we accurately calibrate the full set of parameters of the Heston model. One of the reasons that makes our calibration for short maturities so accurate is that we also take into account the term-structure for large maturities. We may say that calibration is not “memoryless,” in the sense that the option’s behavior far away from maturity does influence calibration when the option gets close to expiration. Our results provide a way to perform a quick calibration of a closed-form approximation to vanilla options that can then be used to price exotic derivatives. The methodology is simple, accurate, fast, and it requires a minimal computational cost.

JEL Classification: G13

Mathematics Subject Classification (2000): 91B28, 91B70

1 Introduction

Although the assumption of constant volatility lends robustness to the Black-Scholes model (see El Karoui, Jeanblanc-Pique and Shreve (1998)), in the last decades the need for more general non-constant volatility models has been the driving force behind numerous works in financial mathematics. One of the reasons behind this driving force is the fact that prices of exotic derivatives based upon the Black-Scholes formula are often inaccurate, as exotic contracts are typically more sensitive to the volatility than vanilla options. Thus, the need was felt for models that could account for the smiles or skews that were often observed in the market.

*Supported by grants ECO2011-288755 and MEC FEDER MTM 2009-08869.

†Supported by grant ECO2009-08302-E.

‡Supported by grants MEC FEDER MTM 2009-08869 and 2009-07203.

One approach to solving this problem has been to let the volatility of the underlying randomly fluctuate according to one or more (correlated) Brownian motions. This approach, started by Hull and White (1987), Wiggins (1987), Stein and Stein (1991) and Heston (1993), has proved to be successful and has evolved over time into a variety of research lines.

A drawback of stochastic volatility models is their increased mathematical complexity, which translates into the difficulty of obtaining closed-form solutions. This, in turn, makes calibration computationally intensive and slow. A recent trend in the literature has been the development of closed-form approximation formulas for option prices (see Fouque, Papanicolau and Sircar (2000), Fouque, Papanicolau, Sircar and Sølna (2003), Hagan, Kumar, Lesniewski and Woodward (2008), DeSantiago, Fouque and Sølna (2008), Antonelli and Scarlatti (2008), Benhamou, Gobet and Miri (2009, 2010a and 2010b), Fouque, Papanicolau, Sircar and Sølna (2011), or Alòs (2012)). The main advantage of closed-form approximations is that they allow for fast calibration and provide a better understanding of the role of model parameters.

Another drawback of stochastic volatility models is that, while they are able to explain volatility smiles and skews for intermediate and long maturities (three months and more), calibration when the options are close to maturity remains unsatisfactory. (See, for example, Janek, Kluge, Weron and Wystup (2010)).

The main purpose of this paper is to present an accurate calibration procedure for very short maturities that requires a minimal computational cost. In Fouque, Papanicolau and Sircar (2000) the authors developed an easy way of identifying the group parameters that are needed for pricing and hedging European-type securities, namely, the average volatility together with the slope and intercept of the implied volatility curve (as a function of the log-moneyness-to-maturity ratio). We build on this way of identifying the parameters, although our approach is slightly different. By applying the results in Alòs (2012) to the Heston model, we deduce a second-order approximation formula for the implied volatility. From the analysis of this approximation we derive valuable information regarding the limiting behavior of the implied volatility. Then, using the term-structure for at-the-money options, we are able to accurately calibrate all model parameters (including the mean-reversion term).

This paper is organized as follows. In Section 2 we briefly describe the model's framework and introduce the basic notation. In Section 3 we present a second-order approximation to the Black-Scholes price based on the results of Alòs (2012). As calibration is typically performed on implied volatilities, in Section 4 we compute a second-order approximation to this magnitude. In Section 5 we present numerical examples in which the parameters are calibrated for the uncorrelated and the correlated cases, and their accuracy is tested on simulated data. In Section 6 our results are compared with those obtained with another calibration procedure (derived by a different method) and conclusions are drawn.

2 Preliminaries and Framework

We consider the following stochastic volatility model for the stock price under a risk neutral probability P chosen by the market:

$$dS_t = rS_t dt + \sigma_t S_t \left(\rho dW_t + \sqrt{1 - \rho^2} dB_t \right), \quad t \in [0, T], \quad (1)$$

where $r \geq 0$ is the constant instantaneous interest rate, W and B are independent standard Brownian motions defined on a complete probability space (Ω, \mathcal{F}, P) , and $\rho \in [-1, 1]$. We will assume that the volatility process σ follows a Heston model (see Heston (1993)), with dynamics governed by

$$d\sigma_t^2 = \kappa(\theta - \sigma_t^2)dt + \nu\sqrt{\sigma_t^2}dW_t, \quad (2)$$

where κ, θ, ν are positive constants satisfying the condition $\frac{2\kappa\theta}{\nu^2} \geq 1$.

We denote by \mathcal{F}^W and \mathcal{F}^B the filtrations generated by W and B , respectively, and we define $\mathcal{F}_t := \mathcal{F}_t^W \vee \mathcal{F}_t^B$. We denote $X_t := \ln S_t$ and $E_t := E(\cdot | \mathcal{F}_t)$. With this notation, the price at time t of a European call with strike K is given by

$$V_t = e^{-r(T-t)} E_t[(e^{X_T} - K)^+]. \quad (3)$$

In what follows we will make use of the following notation:

- $v_t := \sqrt{\frac{1}{T-t} \int_t^T E_t(\sigma_s^2) ds}$ will denote the future average volatility.
- $M_t := \int_0^T E_t(\sigma_s^2) ds$. Notice that $v_t^2 = \frac{1}{T-t}(M_t - \int_0^t \sigma_s^2 ds)$.
- $BS(t, x, \sigma)$ will denote the Black-Scholes price at time t of a European call option with constant volatility σ , current log-stock price x , time to maturity $T - t$, strike price K and interest rate r . We know that in this case

$$BS(t, x, \sigma) = e^x \Phi(d_+) - K e^{-r(T-t)} \Phi(d_-), \quad (4)$$

where Φ denotes the cumulative probability function of the standard normal law and

$$d_{\pm} := \frac{x - x_t^*}{\sigma \sqrt{T-t}} \pm \frac{\sigma}{2} \sqrt{T-t},$$

with $x_t^* := \ln K - r(T-t)$.

- In order to simplify notation, we define

$$\begin{aligned} H(t, x, \sigma) &= (\partial_{xxx}^3 - \partial_{xx}^2) BS(t, x, \sigma) \\ &= \frac{e^x}{\sigma \sqrt{2\pi(T-t)}} \exp\left(-\frac{d_+^2}{2}\right) \left(1 - \frac{d_+}{\sigma \sqrt{T-t}}\right), \end{aligned}$$

and

$$\begin{aligned} K(t, x, \sigma) &= (\partial_{xxxx}^4 - 2\partial_{xxx}^3 + \partial_{xx}^2) BS(t, x, \sigma) \\ &= \frac{e^x}{\sigma \sqrt{2\pi(T-t)}} \exp\left(-\frac{d_+^2}{2}\right) \frac{d_+^2 - \sigma d_+ \sqrt{T-t} - 1}{\sigma^2(T-t)}. \end{aligned}$$

3 Second-order Approximation to the Black-Scholes Price

Our calibration method is built upon the following two results, which provide a second-order approximation to the Black-Scholes price. Both results are proved in Alòs (2012).

Theorem 1 (Decomposition formula) *Under conditions of model (1)-(2) we have*

$$\begin{aligned} V_t &= BS(t, X_t, v_t) \\ &+ \frac{\rho}{2} E_t \left(\int_t^T e^{-r(s-t)} H(s, X_s, v_s) \sigma_s d\langle M, W \rangle \right) \\ &+ \frac{1}{8} E_t \left(\int_t^T e^{-r(s-t)} K(s, X_s, v_s) d\langle M, M \rangle \right). \end{aligned}$$

In order to simplify notation, let $\alpha = \frac{2\kappa\theta}{\nu^2}$, $\beta = \sqrt{2 - \alpha}$, and $\gamma = \sqrt{\frac{5}{2} - \alpha}$.

Theorem 2 (Second-order approximation) *For the model (1)-(2) and for all $t \in [0, T]$ we have the following results, where $C(T, \sigma_t)$ represents a positive constant, non-decreasing as a function of T :*

- If $\alpha \geq \frac{5}{2}$, then

$$\begin{aligned} &\left| V_t - BS(t, X_t, v_t) - \frac{\rho}{2} H(t, X_t, v_t) E_t \left(\int_t^T \sigma_s d\langle M, W \rangle_s \right) \right. \\ &\quad \left. - \frac{1}{8} K(t, X_t, v_t) E_t \left(\int_t^T d\langle M, M \rangle_s \right) \right| \\ &\leq C(T, \sigma_t) \left\{ \nu^2 \rho^2 (T-t)^{\frac{3}{2}} + \nu^3 \rho (T-t)^2 + \nu^4 (T-t)^{5/2} \right\}. \end{aligned}$$

- If $\alpha \in [2, \frac{5}{2})$, then

$$\begin{aligned} & \left| V_t - BS(t, X_t; v_t) - \frac{\rho}{2} H(t, X_t, v_t) E_t \left(\int_t^T \sigma_s d\langle M, W \rangle_s \right) \right. \\ & \quad \left. - \frac{1}{8} K(t, X_t, v_t) E_t \left(\int_t^T d\langle M, M \rangle_s \right) \right| \\ & \leq C(T, \sigma_t) \left\{ \nu^2 \rho^2 (T-t)^{\frac{3}{2}} + \nu^3 \rho (T-t)^2 + \nu^{4-2\gamma} (T-t)^{5/2-2\gamma} \left(\frac{1}{1-\gamma} \right)^{1+\gamma} \right\}. \end{aligned}$$

- If $\alpha \in [\frac{3}{2}, 2)$, then

$$\begin{aligned} & \left| V_t - BS(t, X_t; v_t) - \frac{\rho}{2} H(t, X_t, v_t) E_t \left(\int_t^T \sigma_s d\langle M, W \rangle_s \right) \right. \\ & \quad \left. - \frac{1}{8} K(t, X_t, v_t) E_t \left(\int_t^T d\langle M, M \rangle_s \right) \right| \\ & \leq C(T, \sigma_t) \left\{ \nu^{2(1-\beta)} \left(\frac{1}{1-\beta} \right)^{1+\beta} \left[\rho^2 (T-t)^{\frac{3}{2}(1-\beta)} + \nu \rho (T-t)^{2(1-\beta)} \right] \right. \\ & \quad \left. + \nu^{4-2\gamma} (T-t)^{5/2-2\gamma} \left(\frac{1}{1-\gamma} \right)^{1+\gamma} \right\}. \end{aligned}$$

Although the precision of the bounds in the last theorem has been proved for the short-term (short maturities), our numerical examples show that they also hold for the long-term (see Example 4.6 in Alòs (2012)).

The following results, which are easy to check, are used throughout the paper. In order to facilitate further references, we state them here as a lemma.

Lemma 3 *The following results hold:*

1. $E_t \left(\int_t^T \sigma_s^2 ds \right) = \theta (T-t) + \frac{\sigma_t^2 - \theta}{\kappa} (1 - e^{-\kappa(T-t)})$.
2. $dM_t = \nu \sigma_t \left(\int_t^T e^{-\kappa(r-t)} dr \right) dW_t = \frac{\nu}{\kappa} \sigma_t (1 - e^{-\kappa(T-t)}) dW_t$.
3. $E \left(\int_t^T \sigma_s d\langle M, W \rangle_s \right) = \frac{\nu}{\kappa^2} \left\{ \theta \kappa (T-t) - 2\theta + \sigma_t^2 + e^{-\kappa(T-t)} (2\theta - \sigma_t^2) - \kappa (T-t) e^{-\kappa(T-t)} (\sigma_t^2 - \theta) \right\}$.
4. $E_t \left(\int_t^T d\langle M, M \rangle_s \right) = \frac{\nu^2}{\kappa^2} \left\{ \theta (T-t) + \frac{(\sigma_t^2 - \theta)}{\kappa} (1 - e^{-\kappa(T-t)}) - \frac{2\theta}{\kappa} (1 - e^{-\kappa(T-t)}) - 2(\sigma_t^2 - \theta) (T-t) e^{-\kappa(T-t)} + \frac{\theta}{2\kappa} (1 - e^{-2\kappa(T-t)}) + \frac{(\sigma_t^2 - \theta)}{\kappa} (e^{-\kappa(T-t)} - e^{-2\kappa(T-t)}) \right\}$.

By substituting the above expressions into the approximation formula provided by Theorem 2, we will be able to obtain explicit second-order approximations for the implied volatility. This is what we do in the next section.

4 Second-order Approximation to the Implied Volatility

The market price at time t of a European call option with strike K and maturity T is an observable magnitude, which will be referred to as $BS_t^{obs} = BS^{obs}(t, K, T)$. The *implied volatility* is then defined as the value of the volatility parameter that makes the Black-Scholes price equal to the observed market price. From expression (4) we have that the implied volatility is the value IV that makes:

$$BS(t, x, IV) = BS_t^{obs}.$$

For simplicity, and without loss of generality, we consider $t = 0$. As it is done in Alòs (2012), from the expression in Theorem 2 we deduce a second-order approximation to the implied volatility, \widetilde{IV} , which we will write as

$$\widetilde{IV} = v_0 + I_1 + I_2,$$

with

$$I_1 := \frac{\rho}{2v_0T} \left(1 - \frac{d_+}{v_0\sqrt{T}}\right) E \left(\int_0^T \sigma_s d\langle M, W \rangle_s \right)$$

and

$$I_2 := \frac{1}{8v_0T} \left(\frac{d_+^2}{v_0^2T} - \frac{d_+}{v_0\sqrt{T}} - \frac{1}{v_0^2T} \right) E \left(\int_0^T d\langle M, M \rangle_s \right).$$

The key element that will allow us to calibrate the model's parameters is the limiting behavior of the implied volatility, both close and far away from maturity, together with the term structure for large maturities. We therefore start this section by studying the limiting behavior of \widetilde{IV} . Given that

$$v_0 = \sqrt{\theta + \frac{\sigma_0^2 - \theta}{\kappa T} (1 - e^{-\kappa T})},$$

it is clear that $v_0 \rightarrow \sigma_0$ when $T \rightarrow 0$, and $v_0 \rightarrow \sqrt{\theta}$ when $T \rightarrow \infty$.

As all the results in this section refer to the model (1)-(2), we will only make an explicit reference in the first lemma. From then on, reference to the model will be implicitly assumed.

4.1 Limiting Behavior of I_1

In this section we look at the limit behavior of I_1 . We start by computing the limit of I_1 as the time to maturity goes to 0.

Lemma 4 *Assume the model (1)-(2). Then,*

$$\lim_{T \rightarrow 0} I_1 = -\frac{\rho\nu}{4\sigma_0} (x - \ln K).$$

PROOF. Replacing d_+ by its expression we have:

$$\begin{aligned} \lim_{T \rightarrow 0} I_1 &= \lim_{T \rightarrow 0} \frac{\rho}{2v_0T} \left(1 - \frac{d_+}{v_0\sqrt{T}}\right) E \left(\int_0^T \sigma_s d\langle M, W \rangle_s \right) \\ &= \lim_{T \rightarrow 0} \frac{\rho}{2v_0T} \left(\frac{1}{2} - \frac{r}{v_0^2} \right) E \left(\int_0^T \sigma_s d\langle M, W \rangle_s \right) \\ &\quad - \lim_{T \rightarrow 0} \frac{\rho(x - \ln K)}{2v_0^3T^2} E \left(\int_0^T \sigma_s d\langle M, W \rangle_s \right). \end{aligned}$$

As

$$\begin{aligned} E \left(\int_0^T \sigma_s d \langle M, W \rangle_s \right) &= \nu \int_0^T E(\sigma_s^2) \left(\int_s^T e^{-\kappa(r-s)} dr \right) ds \\ &= \nu \int_0^T \left(\int_0^r e^{-\kappa(r-s)} E(\sigma_s^2) ds \right) dr, \end{aligned}$$

we have

$$\begin{aligned} \lim_{T \rightarrow 0} I_1 &= \lim_{T \rightarrow 0} \frac{\rho\nu}{2v_0 T} \left(\frac{1}{2} - \frac{r}{v_0^2} \right) \int_0^T \left(\int_0^r e^{-\kappa(r-s)} E(\sigma_s^2) ds \right) dr \\ &\quad - \lim_{T \rightarrow 0} \frac{\rho\nu(x - \ln K)}{2v_0^3 T^2} \int_0^T \left(\int_0^r e^{-\kappa(r-s)} E(\sigma_s^2) ds \right) dr. \end{aligned}$$

Applying L'Hôpital rule, it follows that

$$\begin{aligned} \lim_{T \rightarrow 0} I_1 &= \lim_{T \rightarrow 0} \frac{\rho\nu}{2v_0} \left(\frac{1}{2} - \frac{r}{v_0^2} \right) \left(\int_0^T e^{-\kappa(T-s)} E(\sigma_s^2) ds \right) \\ &\quad - \lim_{T \rightarrow 0} \frac{\rho\nu(x - \ln K)}{4v_0^3 T} \left(\int_0^T e^{-\kappa(T-s)} E(\sigma_s^2) ds \right). \end{aligned}$$

The first limit in the right hand side is clearly 0, and the second one is equal to

$$- \lim_{T \rightarrow 0} \frac{\rho\nu(x - \ln K)}{4v_0^3} \left(E(\sigma_T^2) - \kappa e^{-\kappa T} \int_0^T E(\sigma_s^2) e^{\kappa s} ds \right).$$

If we now let $T \rightarrow 0$, the second term of the last equation converges to 0, while the first one converges to

$$- \frac{\rho\nu}{4\sigma_0} (x - \ln K), \quad (5)$$

as we wanted to prove. ■

In the following lemma we explore the behavior of I_1 when the option is far away from maturity.

Lemma 5 *As T increases, the following result holds:*

$$\lim_{T \rightarrow \infty} I_1 = \frac{\rho\nu}{2\kappa} \left(\frac{\sqrt{\theta}}{2} - \frac{r}{\sqrt{\theta}} \right).$$

PROOF. Using the previous computations, we have:

$$\begin{aligned} \lim_{T \rightarrow \infty} I_1 &= \lim_{T \rightarrow \infty} \frac{\rho}{2v_0 T} \left(1 - \frac{d_+}{v_0 \sqrt{T}} \right) E \left(\int_0^T \sigma_s d \langle M, W \rangle_s \right) \\ &= \lim_{T \rightarrow \infty} \frac{\rho\nu}{2v_0} \left(\frac{1}{2} - \frac{r}{v_0^2} \right) e^{-\kappa T} \int_0^T E(\sigma_s^2) e^{\kappa s} ds \\ &\quad - \lim_{T \rightarrow \infty} \frac{\rho\nu(x - \ln K)}{4v_0^3} E(\sigma_T^2) \\ &\quad + \lim_{T \rightarrow \infty} \frac{\rho\nu(x - \ln K)}{4v_0^3} \kappa e^{-\kappa T} \int_0^T E(\sigma_s^2) e^{\kappa s} ds. \end{aligned}$$

It is easy to see that, as $T \rightarrow \infty$, $e^{-\kappa T} \int_0^T E(\sigma_s^2) e^{\kappa s} ds$ converges to $\frac{\theta}{\kappa}$ and $E(\sigma_T^2)$ converges to θ . Therefore, the second and third terms in the last expression vanish and the first one converges to:

$$\frac{\rho\nu}{2\sqrt{\theta}} \left(\frac{1}{2} - \frac{r}{\theta} \right) \frac{\theta}{\kappa} = \frac{\rho\nu}{2\kappa} \left(\frac{\sqrt{\theta}}{2} - \frac{r}{\sqrt{\theta}} \right),$$

and the proof is now complete. ■

4.2 Limiting Behavior of I_2

We now look at the behavior of I_2 , the second-order term of the implied volatility approximation. We start by computing its limit as the time to maturity goes to zero.

Lemma 6 *As we get close to maturity, we have:*

$$\lim_{T \rightarrow 0} I_2 = \frac{\nu^2}{24\sigma_0^3} (x - \ln K)^2.$$

PROOF. We need to compute:

$$\lim_{T \rightarrow 0} I_2 = \lim_{T \rightarrow 0} \frac{1}{8v_0T} \left[\frac{d_+^2}{v_0^2T} - \frac{d_+}{v_0\sqrt{T}} - \frac{1}{v_0^2T} \right] E \left(\int_0^T d \langle M, M \rangle_s \right). \quad (6)$$

On one hand, we have

$$\begin{aligned} \frac{1}{8v_0T} \left[\frac{d_+^2}{v_0^2T} - \frac{d_+}{v_0\sqrt{T}} - \frac{1}{v_0^2T} \right] &= \frac{1}{8v_0^3T^2} (d_+^2 - v_0\sqrt{T}d_+ - 1) \\ &= \frac{1}{8v_0^3T^2} \left[\frac{(x - \ln K)^2}{v_0^2T} + \frac{r^2T}{v_0^2} - \frac{v_0^2T}{4} - 1 \right]. \end{aligned}$$

On the other hand,

$$E \left(\int_0^T d \langle M, M \rangle_s \right) = \frac{\nu^2}{\kappa^2} \int_0^T E(\sigma_s^2) (1 - e^{-\kappa(T-s)})^2 ds.$$

Observe that

$$\left| E \left(\int_0^T d \langle M, M \rangle_s \right) \right| \leq CT,$$

where $C = C(\nu, \kappa, \sigma_0, \theta)$ is a constant. It follows that the limit in (6) is equivalent to:

$$\lim_{T \rightarrow 0} \frac{\nu^2}{8v_0^5T^3} \left[\int_0^T E(\sigma_s^2) \left(\int_s^T e^{-\kappa(r-s)} dr \right)^2 ds \right] (x - \ln K)^2.$$

Applying L'Hôpital rule,

$$\begin{aligned} \lim_{T \rightarrow 0} I_2 &= \lim_{T \rightarrow 0} \frac{\nu^2}{12v_0^5T^2} \left(\int_0^T E(\sigma_s^2) \left(\int_s^T e^{-\kappa(r-s)} dr \right) e^{-\kappa(T-s)} ds \right) (x - \ln K)^2 \\ &= \lim_{T \rightarrow 0} \frac{\nu^2}{12v_0^5T^2} \left(\int_0^T \int_0^T E(\sigma_s^2) e^{-\kappa(r-s)} e^{-\kappa(T-s)} ds dr \right) (x - \ln K)^2 \\ &= \lim_{T \rightarrow 0} \frac{\nu^2}{24Tv_0^5} \left(\int_0^T E(\sigma_s^2) e^{-2\kappa(T-s)} ds \right) (x - \ln K)^2 \\ &= \lim_{T \rightarrow 0} \frac{\nu^2}{24v_0^5} \left(E(\sigma_T^2) - 2\kappa e^{-2\kappa T} \int_0^T E(\sigma_s^2) e^{2\kappa s} ds \right) (x - \ln K)^2 \\ &= \frac{\nu^2}{24\sigma_0^3} (x - \ln K)^2, \end{aligned} \quad (7)$$

which concludes the proof. ■

The next lemma deals with the behavior of I_2 as the time to maturity goes to infinity.

Lemma 7 *As T increases, the following result holds:*

$$\lim_{T \rightarrow \infty} I_2 = \frac{\nu^2 \sqrt{\theta}}{8\kappa^2} \left(\frac{r^2}{\theta^2} - \frac{1}{4} \right).$$

PROOF. We need to compute

$$\lim_{T \rightarrow \infty} \frac{1}{8v_0 T} \left[\frac{d_+^2}{v_0^2 T} - \frac{d_+}{v_0 \sqrt{T}} - \frac{1}{v_0^2 T} \right] E \left(\int_0^T d \langle M, M \rangle_s \right),$$

or, equivalently,

$$\lim_{T \rightarrow \infty} \frac{1}{8v_0^3} \left(\frac{(x - \ln K)^2}{v_0^2 T^3} + \frac{r^2}{v_0^2 T} - \frac{v_0^2}{4T} - \frac{1}{T^2} \right) E \left(\int_0^T d \langle M, M \rangle_s \right).$$

Given that

$$E \left(\int_0^T d \langle M, M \rangle_s \right) \leq CT,$$

the only limit that is not zero as $T \rightarrow \infty$ is

$$\begin{aligned} & \lim_{T \rightarrow \infty} \frac{1}{8v_0} \left(\frac{r^2}{v_0^4} - \frac{1}{4} \right) \frac{1}{T} E \left(\int_0^T d \langle M, M \rangle_s \right) \\ &= \lim_{T \rightarrow \infty} \frac{\nu^2}{8v_0 \kappa^2} \left(\frac{r^2}{v_0^4} - \frac{1}{4} \right) \frac{1}{T} \int_0^T E(\sigma_s^2) \left(1 - e^{-\kappa(T-s)} \right)^2 ds. \end{aligned}$$

Applying L'Hôpital rule, the above limit is equivalent to

$$\lim_{T \rightarrow \infty} \frac{\nu^2}{4v_0 \kappa} \left(\frac{r^2}{v_0^4} - \frac{1}{4} \right) \left(e^{-\kappa T} \int_0^T E(\sigma_s^2) e^{\kappa s} ds - e^{-2\kappa T} \int_0^T E(\sigma_s^2) e^{2\kappa s} ds \right),$$

which is the same as

$$\lim_{T \rightarrow \infty} \frac{\nu^2}{4v_0 \kappa} \left(\frac{r^2}{v_0^4} - \frac{1}{4} \right) \int_0^T (\theta + (\sigma_0^2 - \theta) e^{-\kappa s}) \left(e^{-\kappa(T-s)} - e^{-2\kappa(T-s)} \right) ds.$$

It is straightforward to see that the integral converges to $\frac{\theta}{2\kappa}$. We therefore have that

$$\lim_{T \rightarrow \infty} I_2 = \frac{\nu^2 \sqrt{\theta}}{8\kappa^2} \left(\frac{r^2}{\theta^2} - \frac{1}{4} \right),$$

and the proof is complete. ■

Remark 8 *When the option is close to maturity ($T \rightarrow 0$), the above results allow us to write the second-order approximation to the implied volatility as*

$$\widehat{IV}(0) = \sigma_0 - \frac{\rho\nu}{4\sigma_0} (x - \ln K) + \frac{\nu^2}{24\sigma_0^3} (x - \ln K)^2. \quad (8)$$

Remark 9 *When the option is far away from maturity ($T \rightarrow \infty$), the second-order approximation to the implied volatility becomes*

$$\widehat{IV}(\infty) = \sigma_0 + \frac{\rho\nu}{2\kappa} \left(\frac{\sqrt{\theta}}{2} - \frac{r}{\sqrt{\theta}} \right) + \frac{\nu^2 \sqrt{\theta}}{8\kappa^2} \left(\frac{r^2}{\theta^2} - \frac{1}{4} \right). \quad (9)$$

4.3 Derivatives of \widetilde{IV} when the option is at-the-money

In order to calibrate the model's parameters we will use the implied volatility's term structure. In particular, from the available data we will need to estimate the implied volatility's intercept and slope, and then compute the parameter values that better fit such magnitudes. In this section we therefore derive expressions for the derivatives of \widetilde{IV} at $T = 0$ and at $T = \infty$.

When the option is at-the-money, then $x = x_0^*$ and $d_+ = \frac{v_0}{2}\sqrt{T}$. The expression for \widetilde{IV} thus becomes:

$$\widetilde{IV}(T) = v_0 + \frac{\rho}{4v_0T} E \left(\int_0^T \sigma_s d \langle M, W \rangle_s \right) - \frac{1}{8v_0T} \left(\frac{1}{4} + \frac{1}{v_0^2 T} \right) E \left(\int_0^T d \langle M, M \rangle_s \right). \quad (10)$$

From this expression we can prove the following result.

Lemma 10 *The derivative of the approximation to the implied volatility at $T = 0$ is equal to:*

$$\frac{\partial}{\partial T} \widetilde{IV}(0) = \frac{3\sigma_0^2 \rho \nu - 6\kappa(\sigma_0^2 - \theta) - \nu^2}{24\sigma_0}.$$

PROOF. Using the results from Lemma 3 it is easy to check that $\widetilde{IV}(0) = \sigma_0$. The derivative of \widetilde{IV} with respect to T , at $T = 0$, is therefore equal to:

$$\begin{aligned} \lim_{T \rightarrow 0} \frac{\widetilde{IV}(T) - \sigma_0}{T} &= \lim_{T \rightarrow 0} \frac{v_0 - \sigma_0}{T} \\ &\quad + \lim_{T \rightarrow 0} \frac{\rho}{4v_0T^2} E \left(\int_0^T \sigma_s d \langle M, W \rangle_s \right) \\ &\quad - \lim_{T \rightarrow 0} \frac{1}{8v_0T^2} \left(\frac{1}{4} + \frac{1}{v_0^2 T} \right) E \left(\int_0^T d \langle M, M \rangle_s \right). \end{aligned} \quad (11)$$

For the first term, we have

$$\begin{aligned} \lim_{T \rightarrow 0} \frac{v_0 - \sigma_0}{T} &= \lim_{T \rightarrow 0} \frac{\sqrt{\frac{1}{T} \int_0^T E(\sigma_s^2) ds} - \sigma_0}{T} \\ &= \lim_{T \rightarrow 0} \frac{-\frac{1}{T^2} \int_0^T E(\sigma_s^2) ds - \frac{1}{T} E(\sigma_T^2)}{2\sqrt{\frac{1}{T} \int_0^T E(\sigma_s^2) ds}} \\ &= \lim_{T \rightarrow 0} \frac{-\frac{1}{T^2} \left(\int_0^T E(\sigma_s^2) ds - TE(\sigma_T^2) \right)}{2\sqrt{\frac{1}{T} \int_0^T E(\sigma_s^2) ds}} \\ &= \lim_{T \rightarrow 0} -\frac{1}{2\sigma_0 T^2} \left(\int_0^T E(\sigma_s^2) ds - TE(\sigma_T^2) \right) \\ &= \lim_{T \rightarrow 0} -\frac{1}{2\sigma_0 T^2} \left(\int_0^T E(\sigma_s^2) ds - T(\theta + (\sigma_0^2 - \theta)e^{-\kappa T}) \right) \\ &= \lim_{T \rightarrow 0} -\frac{1}{4\sigma_0 T} \{ E(\sigma_T^2) - (\theta + (\sigma_0^2 - \theta)e^{-\kappa T}) + \kappa T(\sigma_0^2 - \theta)e^{-\kappa T} \} \\ &= -\frac{\kappa(\sigma_0^2 - \theta)}{4\sigma_0} \end{aligned}$$

The second term of equation (11) is equal to:

$$\begin{aligned}
\lim_{T \rightarrow 0} \frac{\rho}{4v_0 T^2} E \left(\int_0^T \sigma_s d \langle M, W \rangle_s \right) &= \frac{\rho \nu}{4\sigma_0} \lim_{T \rightarrow 0} \frac{1}{T^2} \int_0^T E(\sigma_s^2) \left(\int_s^T e^{-\kappa(r-s)} dr \right) ds \\
&= \frac{\rho \nu}{4\sigma_0} \lim_{T \rightarrow 0} \frac{1}{T^2} \int_0^T \left(\int_0^r E(\sigma_s^2) e^{-\kappa(r-s)} ds \right) dr \\
&= \frac{\rho \nu}{8\sigma_0} \lim_{T \rightarrow 0} \frac{1}{T} \int_0^T E(\sigma_s^2) e^{-\kappa(T-s)} ds \\
&= \frac{\rho \nu \sigma_0}{8}.
\end{aligned}$$

Finally, the limit in the third term of expression (11) gives us:

$$\begin{aligned}
\lim_{T \rightarrow 0} \frac{1}{8v_0 T^2} \left(\frac{1}{4} + \frac{1}{v_0^2 T} \right) E \left(\int_0^T d \langle M, M \rangle_s \right) \\
&= \frac{1}{8v_0} \lim_{T \rightarrow 0} \frac{1}{T^2} \left(\frac{1}{4} + \frac{1}{v_0^2 T} \right) E \left(\int_0^T d \langle M, M \rangle_s \right) \\
&= \frac{\nu^2}{8v_0} \lim_{T \rightarrow 0} \frac{1}{T^2} \left(\frac{1}{4} + \frac{1}{v_0^2 T} \right) \int_0^T E(\sigma_s^2) \left(\int_s^T e^{-\kappa(r-s)} dr \right)^2 ds \\
&= \frac{\nu^2}{8v_0} \lim_{T \rightarrow 0} \frac{1}{T^2} \frac{1}{v_0^2 T} \int_0^T E(\sigma_s^2) \left(\int_s^T e^{-\kappa(r-s)} dr \right)^2 ds \\
&= \frac{\nu^2}{8v_0^3} \lim_{T \rightarrow 0} \frac{1}{T^3} \int_0^T E(\sigma_s^2) \left(\int_s^T e^{-\kappa(r-s)} dr \right)^2 ds.
\end{aligned}$$

Applying now L'Hôpital, the above limit is equal to:

$$\begin{aligned}
&\frac{\nu^2}{12v_0^3} \lim_{T \rightarrow 0} \frac{1}{T^2} \int_0^T E(\sigma_s^2) \left(\int_s^T e^{-\kappa(r-s)} dr \right) e^{-\kappa(T-s)} ds \\
&= \frac{\nu^2}{12v_0^3} \lim_{T \rightarrow 0} \frac{1}{T^2} \int_0^T \left(\int_0^r E(\sigma_s^2) e^{-\kappa(r-s)} e^{-\kappa(T-s)} ds \right) dr \\
&= \frac{\nu^2}{24v_0^3} \lim_{T \rightarrow 0} \frac{1}{T} \left(\int_0^T E(\sigma_s^2) e^{-2\kappa(T-s)} ds \right) \\
&= \frac{\nu^2}{24v_0^3} \lim_{T \rightarrow 0} E(\sigma_T^2) - 2\kappa e^{-2\kappa T} \int_0^T E(\sigma_s^2) e^{2\kappa s} ds \\
&= \frac{\nu^2}{24\sigma_0},
\end{aligned}$$

which completes the proof. ■

Remark 11 *When the option is at-the-money, the above result allows us to write the Taylor expansion of \widetilde{IV} near $T = 0$ as:*

$$\widetilde{IV}(T) \approx \sigma_0 + \frac{3\sigma_0^2 \rho \nu - 6\kappa(\sigma_0^2 - \theta) - \nu^2}{24\sigma_0} T. \quad (12)$$

We now compute the derivative of \widetilde{IV} when the option is far away from maturity. In order to prove the next lemma, note that

$$\lim_{T \rightarrow \infty} \widetilde{IV}(T) = \sqrt{\theta} \left(1 + \frac{\nu \rho}{4\kappa} - \frac{\nu^2}{32\kappa^2} \right),$$

which follows easily from (10).

Lemma 12 *As T becomes large (i.e., as the time to maturity increases), the following result holds:*

$$\lim_{T \rightarrow \infty} \left[\widetilde{IV} - \sqrt{\theta} \left(1 + \frac{\nu\rho}{4\kappa} - \frac{\nu^2}{32\kappa^2} \right) \right] T = \frac{\sigma_0^2 - \theta}{2\kappa\sqrt{\theta}} + \nu\rho \frac{\sigma_0^2 - 2\theta}{4\kappa^2\sqrt{\theta}} - \nu^2 \frac{\sigma_0^2 - \frac{5}{2}\theta + 4\kappa}{32\sqrt{\theta}\kappa^3}.$$

PROOF. Note that

$$\begin{aligned} & \lim_{T \rightarrow \infty} \left[\widetilde{IV} - \sqrt{\theta} \left(1 + \frac{\nu\rho}{4\kappa} - \frac{\nu^2}{32\kappa^2} \right) \right] T \\ &= \lim_{T \rightarrow \infty} \left\{ v_0 - \sqrt{\theta} + \frac{\rho}{4v_0T} E \left(\int_0^T \sigma_s d\langle M, W \rangle_s \right) - \frac{\nu\rho\sqrt{\theta}}{4\kappa} \right. \\ & \quad \left. - \frac{1}{8v_0T} \left(\frac{1}{4} + \frac{1}{v_0^2T} \right) E \left(\int_0^T d\langle M, M \rangle_s \right) + \frac{\nu^2\sqrt{\theta}}{32\kappa^2} \right\} T. \end{aligned} \quad (13)$$

Applying L'Hôpital, the first two terms in the limit above give us:

$$\begin{aligned} \lim_{T \rightarrow \infty} (v_0 - \sqrt{\theta}) T &= \lim_{T \rightarrow \infty} \frac{\sqrt{\frac{1}{T} \int_0^T E(\sigma_s^2) ds} - \sqrt{\theta}}{1/T} \\ &= \lim_{T \rightarrow \infty} \frac{\frac{1}{T^2} \left\{ \int_0^T E(\sigma_s^2) ds - TE(\sigma_T^2) \right\}}{2v_0(1/T^2)} \\ &= \lim_{T \rightarrow \infty} \frac{1}{2v_0} \left(\theta T + \frac{\sigma_0^2 - \theta}{\kappa} (1 - e^{-\kappa T}) - T\theta - T(\sigma_0^2 - \theta) e^{-\kappa T} \right) \\ &= \frac{\sigma_0^2 - \theta}{2\kappa\sqrt{\theta}}. \end{aligned}$$

We now consider the next two terms in the right-hand side of expression (13). Using Lemma 3 it follows that

$$\begin{aligned} & \lim_{T \rightarrow \infty} \left\{ \frac{\rho}{4v_0} E \left(\int_0^T \sigma_s d\langle M, W \rangle_s \right) - \frac{\nu\rho\sqrt{\theta}}{4\kappa} T \right\} \\ &= \lim_{T \rightarrow \infty} \left\{ \frac{\nu\rho}{4\kappa^2v_0} (\kappa\theta T - 2\theta + \sigma_0^2 + [2\theta - \sigma_0^2 - \kappa T(\sigma_0^2 - \theta)] e^{-\kappa T}) - \frac{\nu\rho\sqrt{\theta}}{4\kappa} T \right\} \\ &= \frac{\nu\rho}{4\kappa^2\sqrt{\theta}} (\sigma_0^2 - 2\theta). \end{aligned}$$

Applying Lemma 3 again, the last two terms in the right-hand side of (13) give us:

$$\begin{aligned} & \lim_{T \rightarrow \infty} \left\{ -\frac{1}{8v_0} \left(\frac{1}{4} + \frac{1}{v_0^2T} \right) E \left(\int_0^T d\langle M, M \rangle_s \right) + \frac{\nu^2\sqrt{\theta}}{32\kappa^2} T \right\} \\ &= \lim_{T \rightarrow \infty} \left\{ -\frac{1}{32v_0} E \left(\int_0^T d\langle M, M \rangle_s \right) + \frac{\nu^2\sqrt{\theta}}{32\kappa^2} T - \frac{1}{8v_0^3T} E \left(\int_0^T d\langle M, M \rangle_s \right) \right\} \\ &= \lim_{T \rightarrow \infty} \left\{ -\frac{\nu^2}{32v_0\kappa^2} \left[\theta T + \frac{\sigma_0^2 - \theta}{\kappa} - \frac{2\theta}{\kappa} + \frac{\theta}{2\kappa} \right] + \frac{\nu^2\sqrt{\theta}}{32\kappa^2} T - \frac{\nu^2}{8v_0^3\kappa^2} \theta \right\} \\ &= -\frac{\nu^2}{32\sqrt{\theta}\kappa^3} \left(\sigma_0^2 - \frac{5}{2}\theta + 4\kappa \right). \end{aligned}$$

Putting these limits together, we get that

$$\lim_{T \rightarrow \infty} \left[\widetilde{IV} - \sqrt{\theta} \left(1 + \frac{\nu\rho}{4\kappa} - \frac{\nu^2}{32\kappa^2} \right) \right] T = \frac{\sigma_0^2 - \theta}{2\kappa\sqrt{\theta}} + \nu\rho \frac{\sigma_0^2 - 2\theta}{4\kappa^2\sqrt{\theta}} - \nu^2 \frac{\sigma_0^2 - \frac{5}{2}\theta + 4\kappa}{32\sqrt{\theta}\kappa^3},$$

which is the desired result. ■

Remark 13 *The above result allows us to conclude that, for an at-the-money European call option which is far away from maturity, the following approximation holds:*

$$\widetilde{IV}(T) \approx \sqrt{\theta} \left(1 + \frac{\nu\rho}{4\kappa} - \frac{\nu^2}{32\kappa^2} \right) + \left(\frac{\sigma_0^2 - \theta}{2\kappa\sqrt{\theta}} + \nu\rho \frac{\sigma_0^2 - 2\theta}{4\kappa^2\sqrt{\theta}} - \nu^2 \frac{\sigma_0^2 - \frac{5}{2}\theta + 4\kappa}{32\sqrt{\theta}\kappa^3} \right) \frac{1}{T}. \quad (14)$$

5 Calibration

In this section we test the accuracy of our results by calibrating the model from simulated data. Let $S_0 = 100$, $\sigma_0 = 0.2$, $\kappa = 3$, $\nu = 0.3$, $\rho = 0$, $r = 0$, and $\theta = 0.09$. From the model equations, we first generate option prices for small and large maturities and we then invert them in order to get the corresponding (at-the-money) implied volatilities. When we say ‘‘short maturities’’ we roughly refer to $T = 0.01$ to 0.05 years, while ‘‘large maturities’’ means $T = 3$ to 4 years.

Before moving on to numerical examples, we offer a bird’s-eye view of the calibration procedure. The first step is to plot the implied volatilities for short maturities as a function of T and to fit a curve to the data. From expression (12) we obtain σ_0 as the intercept of the fitted equation. The second step, which also follows from (12), consists of making

$$\frac{-\kappa(\sigma_0^2 - \theta)}{4\sigma_0} + \frac{\rho\nu\sigma_0}{8} - \frac{\nu^2}{24\sigma_0}$$

equal to the slope of the regression curve.

The third step is to plot the implied volatilities for short maturities as a function of the log-moneyness $(x - \ln K)$ and fit a curve to the data. The product $\nu\rho$ is obtained, according to (8), from the coefficient of the linear term in the regression equation.

The fourth step consists of plotting the implied volatilities as a function of $1/T$ for large values of T and fitting a curve to the data. Using expression (14), we then make

$$\sqrt{\theta} \left(1 + \frac{\nu\rho}{4\kappa} - \frac{\nu^2}{32\kappa^2} \right)$$

and

$$\frac{\sigma_0^2 - \theta}{2\kappa\sqrt{\theta}} + \nu\rho \frac{\sigma_0^2 - 2\theta}{4\kappa^2\sqrt{\theta}} - \nu^2 \frac{\sigma_0^2 - \frac{5}{2}\theta + 4\kappa}{32\sqrt{\theta}\kappa^3}$$

equal to the intercept and the slope, respectively, of the regression curve.

The final step is to solve the system of equations generated in the second and fourth steps, using the information gathered in the first and third steps. We consider two cases, the uncorrelated one ($\rho = 0$) and the correlated one ($\rho \neq 0$).

5.1 The uncorrelated case ($\rho = 0$)

In Figure 1 we plot the different implied volatilities obtained from the simulated prices against the corresponding maturities (expressed in years). By running a regression, we get that the intercept is 0.2 and the slope of the linear term is 0.1676.

When the option is at-the-money, the implied volatility at $T = 0$ is σ_0 . Using a hat to designate calibrated magnitudes, we thus write $\widehat{\sigma}_0 = 0.2$. From expression (12) it follows that

$$\frac{3\widehat{\sigma}_0^2\rho\nu - 6\kappa(\widehat{\sigma}_0^2 - \theta) - \nu^2}{24\widehat{\sigma}_0} \approx 0.1676,$$

or, equivalently,

$$0.12\rho\nu - 6\kappa(0.04 - \theta) - \nu^2 \approx 0.80448.$$

We now look at the implied volatility as a function of the log-moneyness $(x - \ln K)$. It follows from expressions (5) and (7) that, for short maturities, the implied volatility tends to

$$\sigma_0 - \frac{\nu\rho}{4\sigma_0} (x - \ln K) + \frac{\nu^2}{24\sigma_0^3} (x - \ln K)^2.$$

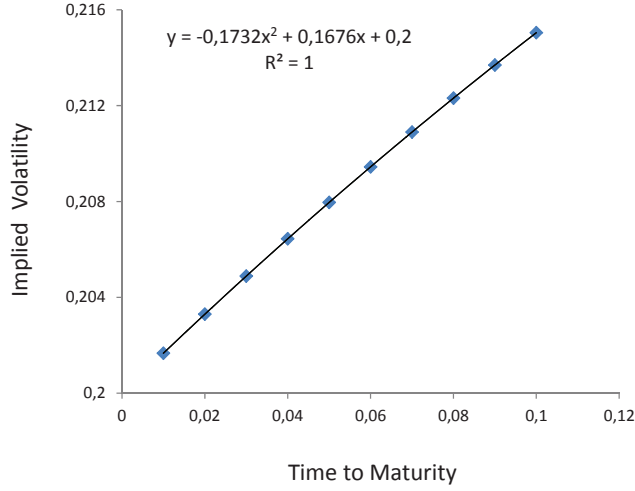


Figure 1: *Implied Volatility when the at-the-money option is close to maturity. (In this and the remaining figures, time to maturity is expressed in years).*

In Figure 2 we plot the implied volatilities against the log-moneyness. By running a regression, we get that the coefficient of the first order term is zero (4×10^{-7}), which gives $\nu\rho = 0$.

Note that the regression coefficient of the second order term is 0.443, from where one could be tempted to conclude that $\hat{\nu} = \sqrt{24 \times 0.443 \times 0.2^3} = 0.29164$. However, calibration of the second-order coefficient from the above equation can be unstable, for it depends on the correct estimation of the implied volatility for strikes that are out-of-the-money. We therefore consider 0.29164 only as a rough approximation to the value of ν . We will see below that a more accurate calibration of this parameter requires the use of the term-structure for long maturities.

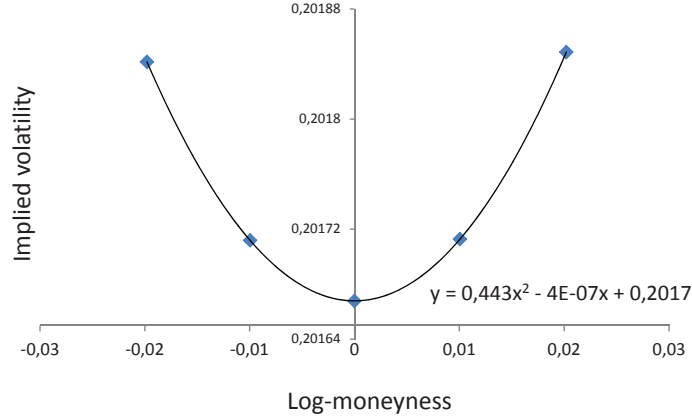


Figure 2: *Implied Volatility as a function of log-moneyness for short maturities.*

The next step is to gather additional information from the implied volatility. We know from (14) that, for large values of T , the implied volatility is approximately equal to:

$$\sqrt{\theta} \left(1 + \frac{\nu\rho}{4\kappa} - \frac{\nu^2}{32\kappa^2} \right) + \left(\frac{\sigma_0^2 - \theta}{2\kappa\sqrt{\theta}} + \nu\rho \frac{\sigma_0^2 - 2\theta}{4\kappa^2\sqrt{\theta}} - \nu^2 \frac{\sigma_0^2 - \frac{5}{2}\theta + 4\kappa}{32\sqrt{\theta}\kappa^3} \right) \frac{1}{T}.$$

By performing a regression on the data from Figure 3, we get that the intercept is

$$\sqrt{\theta} \left(1 + \frac{\nu\rho}{4\kappa} - \frac{\nu^2}{32\kappa^2} \right) \approx 0.2998,$$

while the slope is

$$\frac{\sigma_0^2 - \theta}{2\kappa\sqrt{\theta}} + \nu\rho \frac{\sigma_0^2 - 2\theta}{4\kappa^2\sqrt{\theta}} - \nu^2 \frac{\sigma_0^2 - \frac{5}{2}\theta + 4\kappa}{32\sqrt{\theta}\kappa^3} \approx -0.0314.$$

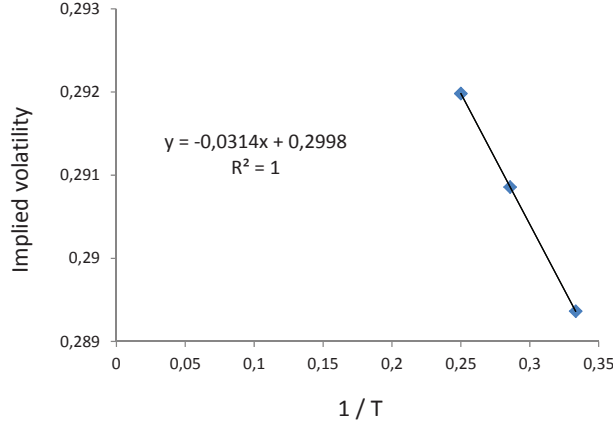


Figure 3: *Implied Volatility as a function of 1/T.*

Putting everything together, we have the following system:

$$\left. \begin{aligned} -6\kappa(0.04 - \theta) - \nu^2 &\approx 0.80448 \\ \sqrt{\theta} \left(1 - \frac{\nu^2}{32\kappa^2} \right) &\approx 0.2998 \\ \frac{0.04 - \theta}{2\kappa\sqrt{\theta}} - \nu^2 \frac{0.04 - \frac{5}{2}\theta + 4\kappa}{32\sqrt{\theta}\kappa^3} &\approx -0.0314 \end{aligned} \right\}.$$

Solving the system we find that the calibrated values of the parameters are as in the table below (where the error is expressed in absolute value).

parameter	real	calibrated	error
σ_0	0.2	0.2	0%
ν	0.3	0.3020	0.67%
κ	3	3.0439	1.46%
θ	0.09	0.0899	0.07%

5.2 The correlated case ($\rho \neq 0$)

Recall that when the option is at-the-money, the implied volatility at $T = 0$ is σ_0 . We also have from Lemma 10 that the derivative of the volatility at $T = 0$ is

$$\frac{-\kappa(\sigma_0^2 - \theta)}{4\sigma_0} + \frac{\rho\nu\sigma_0}{8} - \frac{\nu^2}{24\sigma_0}.$$

In Figure 4 we plot the implied volatilities obtained from the simulated prices against the corresponding maturities, as in the previous example. By running a regression, we see that the intercept is 0.2, which gives $\hat{\sigma}_0 = 0.2$.

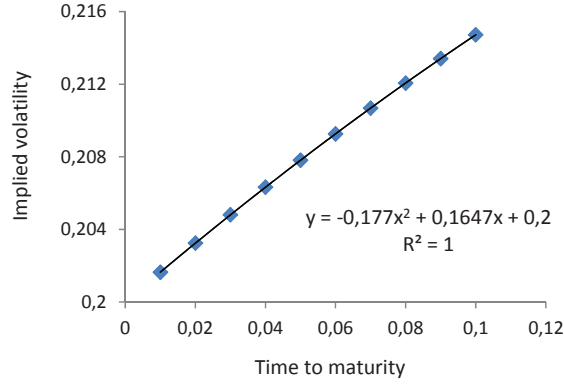


Figure 4: *Implied Volatility as a function of time to maturity.*

As the first-order coefficient is equal to 0.1647, equation (12) allows us to write

$$\frac{-\kappa(\sigma_0^2 - \theta)}{4\sigma_0} + \frac{\rho\nu\sigma_0}{8} - \frac{\nu^2}{24\sigma_0} \approx 0.1647.$$

We now look at the implied volatility as a function of the log-moneyness $(x - \ln K)$. From expressions (5) and (7) we know that, for short maturities, the implied volatility tends to

$$\sigma_0 - \frac{\nu\rho}{4\sigma_0}(x - \ln K) + \frac{\nu^2}{24\sigma_0^3}(x - \ln K)^2.$$

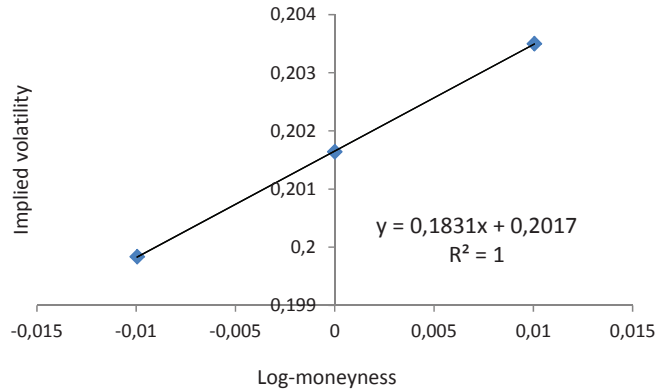


Figure 5: *Implied Volatility as a function of log-moneyness for short maturities.*

In Figure 5 we plot the implied volatilities against the log-moneyness. Note that the plot is strongly linear, which makes it difficult to estimate the second-order coefficient. As the coefficient of the first-order term is equal to 0.1831, it follows from the last equation that $\widehat{\nu\rho} = -0.14648$.

The next step is to gather additional information from the (at-the-money) implied volatility. We know from (14) that, for large values of T , the implied volatility is approximately equal to:

$$\sqrt{\theta} \left(1 + \frac{\nu\rho}{4\kappa} - \frac{\nu^2}{32\kappa^2} \right) + \left(\frac{\sigma_0^2 - \theta}{2\kappa\sqrt{\theta}} + \nu\rho \frac{\sigma_0^2 - 2\theta}{4\kappa^2\sqrt{\theta}} - \nu^2 \frac{\sigma_0^2 - \frac{5}{2}\theta + 4\kappa}{32\sqrt{\theta}\kappa^3} \right) \frac{1}{T}.$$

By performing a regression on the data from Figure 6, we get that

$$\begin{aligned} \sqrt{\theta} \left(1 + \frac{\nu\rho}{4\kappa} - \frac{\nu^2}{32\kappa^2} \right) &\approx 0.2961 \\ \frac{\sigma_0^2 - \theta}{2\kappa\sqrt{\theta}} + \nu\rho \frac{\sigma_0^2 - 2\theta}{4\kappa^2\sqrt{\theta}} - \nu^2 \frac{\sigma_0^2 - \frac{5}{2}\theta + 4\kappa}{32\sqrt{\theta}\kappa^3} &\approx -0.0303. \end{aligned}$$

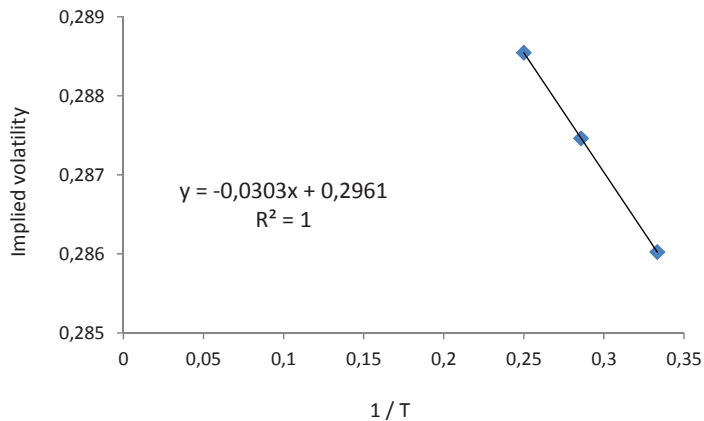


Figure 6: *Implied Volatility as a function of 1/T.*

Putting everything together, we have the following system:

$$\left. \begin{aligned} -0.12 \cdot 0.14624 - 6\kappa(0.04 - \theta) - \nu^2 &\approx 0.158112 \\ \sqrt{\theta} \left(1 - \frac{0.14624}{4\kappa} - \frac{\nu^2}{32\kappa^2} \right) &\approx 0.2961 \\ \frac{0.04 - \theta}{2\kappa\sqrt{\theta}} - 0.14624 \frac{0.04 - 2\theta}{4\kappa^2\sqrt{\theta}} - \nu^2 \frac{0.04 - \frac{5}{2}\theta + 4\kappa}{32\sqrt{\theta}\kappa^3} &\approx -0.0303 \end{aligned} \right\}.$$

Solving it (taking into account that $\widehat{\nu\rho} = -0.14648$), we get that the calibrated values provide a fairly accurate estimate of the real parameter values, as can be seen in the table below (the errors are expressed in absolute value).

parameter	real	calibrated	error
σ_0	0.2	0.2	0%
ν	0.3	0.2997	0.11%
κ	3	3.0023	0.08%
θ	0.09	0.08985	0.17%
ρ	-0.5	-0.488	2.24%

6 Summary and Conclusions

In this paper we have presented a calibration procedure for very short maturities in the context of the Heston model. When applied to simulated data, this method allows us to calibrate the full set of Heston parameters $(\sigma_0, \nu, \kappa, \theta, \rho)$. Our results provide a way to perform a quick and accurate calibration of a closed-form approximation to the price of vanilla options that can then be used to price exotic derivatives.

As a way to illustrate the method's accuracy, we compare our results with those recently reported by Forde, Jacquier and Lee (2011). Their method, different than ours, is based on saddlepoint expansions in the complex plane and the properties of holomorphic functions. They consider a Heston model with parameter values $\sigma_0 = 0.2$, $\nu = 0.2$, $\kappa = 1.15$, $\theta = 0.04$ and $\rho = -0.4$. In the table below we present the calibrated values of the parameters obtained with our method, together with those reported by Forde, Jacquier and Lee (2011).

parameter	our			Forde et al.	
	real	calibration	error	calibration ¹	error
σ_0	0.2	0.2	0%	—	—
ν	0.2	0.1945	2.75%	0.1907	4.65%
κ	1.15	1.1688	1.63%	1.1040	4.00%
θ	0.04	0.0399	0.25%	0.0410	2.5%
ρ	-0.4	-0.4072	1.80%	-0.4069	1.73%

One of the reasons that makes our calibration so accurate is the fact that we make use of the term-structure for large maturities (i.e., the region of the volatility surface that is far away from maturity), while Forde, Jacquier and Lee (2011) only consider the short term. We may thus say that calibration is not “memoryless,” in the sense that the option’s behavior far away from maturity does influence calibration when the option gets close to expiration.

The main traits of the calibration methodology that has been presented in this paper are simplicity, accuracy, and speed: the procedure is fast to implement and it requires a minimal computational cost. By including the term-structure for large maturities we are able to considerably improve its accuracy.

References

- [1] E. Alòs (2012): *A decomposition formula for option prices in the Heston model and applications to option pricing approximation*. To appear in *Finance and Stochastics*.
- [2] F. Antonelli and S. Scarlatti (2009): *Pricing options under stochastic volatility: a power series approach*. *Finance and Stochastics* 13 (2): 269-303.
- [3] E. Benhamou, E. Gobet and M. Miri (2009): *Smart expansion and fast calibration for jump diffusion*. *Finance and Stochastics* 13 (4): 563-589.
- [4] E. Benhamou, E. Gobet and M. Miri (2010a): *Expansion formulas for European options in a local volatility model*. *International Journal of Theoretical and Applied Finance* 13 (4): 603-634.
- [5] E. Benhamou, E. Gobet and M. Miri (2010b): *Time dependent Heston model*. *SIAM Journal on Financial Mathematics* 1: 289-325.
- [6] R. DeSantiago, J. P. Fouque and K. Sølna (2008): *Bond Markets with Stochastic Volatility*. *Advances in Econometrics* 22: 215-242
- [7] N. El Karoui, M. Jeanblanc-Pique and S. Shreve (1998): *Robustness of Black and Scholes Formula*. *Mathematical Finance* 8: 93-126.
- [8] M. Forde, A. Jacquier and R. Lee (2011): *The Small-Time Smile and Term Structure of Implied Volatility under the Heston Model*. *SIAM Journal of Financial Mathematics*. To appear.
- [9] J. P. Fouque, G. Papanicolau and K. R. Sircar (2000): *Derivatives in Financial markets with Stochastic Volatility*. Cambridge.
- [10] J. P. Fouque, G. Papanicolau, K. R. Sircar and K. Sølna (2003): *Singular Perturbations in Option Pricing*. *SIAM Journal of Applied Mathematics* 63 (5): 1648-1665.
- [11] J. P. Fouque, G. Papanicolau, K. R. Sircar and K. Sølna (2011): *Multiscale Stochastic Volatility for Equity, Interest Rate, and Credit Derivatives*. Cambridge.
- [12] P. S. Hagan, D. Kumar, A. Lesniewski and D. E. Woodward (2002): *Managing smile risk*. *Willmott magazine* 15: 84-108.

¹ Forde, Jacquier and Lee (2011) do not calibrate σ_0 .

- [13] S. L. Heston (1993): *A closed-form solution for options with stochastic volatility with applications to bond and currency options*. *Review of Financial Studies* 6 (2): 327-343.
- [14] J. C. Hull and A. White (1987): *The pricing of options on assets with stochastic volatilities*. *Journal of Finance* 42: 281-300.
- [15] A. Janek, T. Kluge, R. Weron and U. Wystup (2010): *FX smile in the Heston Model*. Humboldt University, SFB 649 Discussion Paper 2010-047.
- [16] E. M. Stein and J. C. Stein (1991): *Stock price distributions with stochastic volatility: An analytic approach*. *The Review of Financial Studies* 4: 727-752.
- [17] J. Wiggins (1987): *Option values under stochastic volatilities*. *Journal of Financial Economics*, 19: 351-372.